Accuracy of mandibular force profiles for bite force estimation and feeding behavior reconstruction in extant and extinct carnivorans

François Therrien[1,2,*], Annie Quinney[3], Kohei Tanaka[2], and Darla K. Zelenitsky[2]

[1] Royal Tyrrell Museum of Palaeontology, PO Box 7500, Drumheller, AB, T0J 0Y0, Canada

[2] Department of Geoscience, University of Calgary, 2500 University Drive NW, Calgary, AB, T2N 1N4, Canada

[3] Arctic Institute of North America, University of Calgary, 2500 University Drive NW, Calgary, AB, T2N 1N4, Canada

*Corresponding author: francois.therrien@gov.ab.ca

Keywords: beam theory, mandible, feeding behavior, bite force, Carnivora, computed tomography

Summary statement:
Computed tomography reveals that mandibular force profiles permit highly accurate reconstruction of bite force and feeding behavior in extant and extinct carnivorans.

ABSTRACT

Mandibular force profiles apply the principles of beam theory to identify mandibular biomechanical properties that reflect the bite force and feeding strategies of extant and extinct predators. While this method uses external dimensions of the mandibular corpus to determine its biomechanical properties, more accurate results could potentially be obtained by quantifying its internal cortical bone distribution. To test this possibility, mandibular force profiles were calculated using both external mandibular dimensions ('solid mandible model') and quantification of internal bone distribution of the mandibular corpus obtained from CT scans ('hollow mandible model') for five carnivorans (*Canis lupus*, *Crocuta crocuta*, *Panthera leo*, *Neofelis nebulosa*, and the extinct *Canis dirus*). Comparison reveals that the solid model slightly overestimates mandibular biomechanical properties, but the pattern of change in biomechanical properties along the mandible remains the same. As such, feeding behavior reconstructions are consistent between the two models and are not improved by computed tomography. Bite force estimates produced by the two models are similar, except for *Crocuta* where the solid model underestimates bite force by 10%-14%. This discrepancy is due to the more solid nature of the *Crocuta* mandible relative to other carnivorans. Therefore, computed tomography improves bite force estimation accuracy for taxa with thicker mandibular corpora, but not significantly so otherwise. Bite force estimates derived from mandibular force profiles are far closer to empirically-measured bite force than those inferred from jaw musculature dimension. Consequently, bite force estimates derived from this method can be used to calibrate finite-element analysis models.

Journal of Experimental Biology • Advance article

INTRODUCTION

Feeding behaviour and bite force are significant aspects of the ecology of a predator, as both play an important role in determining the type/size of prey hunted and the trophic position of the predator (Meers, 2002; Verwaijen et al., 2002; Wroe et al., 2005; Van Valkenburgh, 2007; see also Jonathan H. Wiersma, Maximum estimated bite force, skull morphology, and primary prey size in North American carnivores, M.Sc. thesis, Laurentian University, 2001). Feeding behavior in extinct predators is usually inferred from the study of their craniomandibular characteristics and dental morphology, which can be interpreted as adaptations for capturing prey and processing food. Various approaches applying biomechanical principles based on beam theory (e.g., Biknevicius and Ruff, 1992a; Therrien, 2005a,b; Organ et al., 2006) have been developed to investigate and compare the feeding behaviors and bite capabilities of extant and extinct mammalian predators jaw musculature reconstructions (e.g., Christiansen and Adolfssen, 2005; Wroe et al. 2005; Christiansen and Wroe, 2007), or finite-element analysis (FEA; e.g., McHenry et al., 2007; Slater et al., 2009, 2010; Tseng and Binder, 2010; Tseng and Wang, 2010; Tseng et al., 2011; Jones et al., 2013; Tseng, 2013; Wroe et al. 2013; Figueirido et al., 2014). Although most methods require exquisitely preserved specimens (i.e., complete or undistorted specimens) and/or extensive computational facilities (i.e., access to CT scanners and bioengineering software), the mandibular force profile method is simpler and has the advantages of being easily reproducible, widely applicable to various taxa, and requiring only access to isolated mandibles (e.g., Therrien 2005a,b; Therrien et al., 2005; Christiansen, 2007; Blanco et al., 2011; Jasinski, 2011).

Mandibular force profiles apply beam theory to determine the biomechanical properties of mandibles, which reflect the loads and stresses endured by mandibles during life (Biknevicius and Ruff, 1992a; Therrien, 2005a,b; Therrien et al., 2005). This approach follows the assumption that bone has evolved to achieve maximum strength with a minimum amount of material and to remodel itself in response to the loads to which it is subjected. Reflecting this notion, both cortical thickness and bone shape will reflect the habitual loads experienced during life: elliptical shapes characterize bones that undergo higher bending stresses in one direction over another whereas greater cortical thickness characterizes bones subjected to high loads (see Wainwright et al., 1982; Lanyon and Rubin, 1985). Mandibular force profiles use the external dimensions of mandibles to model mandibles as solid, elliptical beams composed of cortical bone that undergo bending loads during ingestion, here termed the ‘solid mandible model’ (Fig. 1; equivalent to the ‘solid symmetrical model’ of

Biknevicius and Ruff, 1992b). However, mandibles modeled as solid ellipses may poorly reflect the mandible capacity to withstand bending stresses for three reasons: 1) the mandibular corpus contains porous cancellous bone, thus making it partly hollow, 2) the amount of cancellous bone in the mandibular cross-section varies along the mandible and between taxa, and 3) the cross-section of a mandible may differ from a perfect elliptical shape (see Biknevicius and Ruff, 1992b). As such, these divergences could lead to erroneous estimation of the biomechanical properties of the mandible, resulting in the misinterpretation of feeding behavior and bite force.

More accurate determination of mandibular biomechanical properties can potentially be achieved by quantifying the amount and distribution of cortical bone in the cross-section of the mandibular corpus through the use of x-ray imagery and computed tomography (CT) scans (Biknevicius and Ruff, 1992b). To investigate the impact of x-ray imagery on the accuracy of mandibular force profiles, mandibles of extant and extinct carnivorans were CT scanned to quantify the internal distribution of cortical bone in the mandibular corpus in order to derive revised mandibular force profiles, an approach here termed the 'hollow mandible model' (Fig. 1). These results were compared to mandibular force profiles derived from external mandibular dimensions measured on the same CT data (i.e., "solid mandible model") in order to determine: 1) whether feeding behaviour interpretations differ between the two models, and 2) whether the hollow mandible model provides more accurate bite force estimates than the solid mandible model. As such, this study will determine whether the use of computed tomography significantly affects paleoecological interpretations inferred from the mandibular force profiles derived from external measurements.

LIST OF SYMBOLS AND ABBREVIATIONS

M_3: 3rd molar; M_2: 2nd molar; M_1: 1st molar (carnassial); P_4: 4th premolar; P_3: 3rd premolar; P_2: 2nd premolar; Ix: second moment of area about the mediolateral axis; Iy: second moment of area about the dorsoventral axis; Zx: section modulus about the mediolateral axis; Zy: section modulus about the dorsoventral axis; Zx/L: dorsoventral mandibular force; Zx/Zy: relative mandibular force (or overall mandibular shape); CA: cortical bone area in mandibular cross-section; TA: total area of mandibular cross-section; USNM: United States National Museum of Natural History, Smithsonian Institute, Washington, D.C.

MATERIALS & METHODS

Samples

Dentaries of five carnivoran species (*Panthera leo*, *Neofelis nebulosa*, *Crocuta crocuta*, *Canis lupus*, and the extinct *Canis dirus*†), each represented by two large adult specimens (Table 1), were scanned on a Siemens Somatom CT scanner (slice thickness 1 mm, pixel dimension was 0.2 mm, energy and current levels were not recorded but presumably close to the standards of 120 kV and 200 mA for CT scanning specimens; see Ridgely and Witmer, 2006) in the Department of Anthropology at the National Museum of Natural History, Washington, D.C. The ramus was oriented in life position and CT scans were selectively made at each individual interdental gap in the coronal plane, perpendicular to the neutral axis (which is approximated by the central axis) of the mandible (Fig. 2). At the canine, CT scans were taken diagonally from the lingual aspect of the symphysis through the posterior margin of the canine alveolus so the CT slices were taken perpendicular to the neutral axis of the mandible. The distance between each interdental gap and the middle of the articular condyle (L) was measured with calipers.

Individual CT slices were saved as IMA files and analyzed using the software ImageJ v. 1.40g. Mandibular depth and width, defined as the greatest diameter of the mandibular corpus in the vertical and horizontal planes, respectively, were measured in each CT slice with the ImageJ measuring tool (Fig. 1). A few CT slices were edited in ImageJ to better define the extent of cortical bone (with white paintbrush tool), erase cancellous bone and tooth crowns (with black paintbrush tool), and fill tooth alveoli for analytical purposes (with white paintbrush tool). When the distinction between cortical bone and medullary cavity was difficult to determine in a CT slice, comparison with the CT slice for the same interdental gap in the second individual of the same species was made in order to delineate the extent of the cortical bone. Biomechanical properties (see below), total surface area (TA) of the mandibular corpus cross-section, and surface area represented by cortical bone (CA) in the mandibular corpus cross-section were quantified in each CT slice using the MomentMacro version 1.3 (freely available at http://www.hopkinsmedicine.org/FAE/mmacro.htm) run within ImageJ.

Mandibular force profiles

Following the principles of beam theory, mandibles can be modeled as cantilevers undergoing bending loads during food ingestion (for a review, see Therrien, 2005a and Therrien et al., 2005). Biomechanical properties of the mandible are calculated based on the dimensions of the mandibular corpus and the distribution of cortical bone within it (Biewener, 1992; Biknevicius and Ruff, 1992a). In this study, the second moment of area (I), a measure of bone distribution around a given axis, is evaluated in two different ways: 1) using measurements of the vertical (i.e., dorsoventral) and horizontal (i.e., labiolingual) diameters of the mandibular corpus, which assumes that the latter has a solid elliptical cross-section (*sensu* the solid mandible model, see Fig. 1); and 2) through quantification (via the MomentMacro) of cortical bone distribution in the mandibular corpus based on CT scan images, which takes into consideration the actual shape of the mandibular corpus cross-section (i.e., any deviation from a perfect elliptical cross-section) and the presence of cancellous bone in the corpus (*sensu* the hollow mandible model, see Fig. 1). Because the hollow mandible model takes into consideration the actual shape of and the internal distribution of cortical bone in the mandibular corpus, its results are considered to represent the true biomechanical properties of the mandible (see Biknevicius and Ruff, 1992b).

From the second moment of area, the following properties were evaluated for both solid and hollow mandible models at each interdental gap:

1) Zx: Section modulus or maximum bending strength about the mediolateral axis
    - for the solid ellipse model: $Zx = \pi * (\text{mandibular width}/2) * (\text{mandibular depth}/2)^2 / 4$
    - for the hollow mandible model: Zx = Ix / (mandibular depth/2), where Ix is the second moment of area determined by MomentMacro.
2) Zy: Section modulus or maximum bending strength about the dorsoventral axis
    - for the solid ellipse model: $Zy = \pi * (\text{mandibular depth}/2) * (\text{mandibular width}/2)^2 / 4$
    - for the hollow mandible model: Zy = Iy / (mandibular width/2) , where Iy is the second moment of area determined by MomentMacro.
3) Zx/L: Dorsoventral mandibular force. By assuming constancy of bone material property and safety factor in the vertebrate mandible, the flexure formula of Timoshenko and Gere (1972) can be modified to show that the applied force on a

structure can be expressed as the ratio of the section modulus over the moment arm length (for details, see Therrien, 2005a). As such, Zx/L is a measure of the maximum force applied in the dorsoventral plane at an interdental gap, where L is the distance separating the interdental gap studied from the articular condyle;

4) Zx/Zy: Relative mandibular force (or overall mandibular shape) at a given point.
5) CA/TA: Ratio of cortical bone area to total surface area of the mandibular corpus cross-section; a measure of the "hollowness" of the mandible at a given interdental gap.

Species means were calculated for each of the aforementioned variables. For the hollow mandible model, species means were calculated from the values produced by MomentMacro. For the solid mandible model, linear measurements (mandibular depth, mandibular width, and distance to interdental gaps) of both individuals of a given species were averaged prior to calculating the mandibular biomechanical properties. The graphic representations of variations in biomechanical properties, namely bending force (Z/L) and relative mandibular force (Zx/Zy), along the mandible are called mandibular force profiles and have been shown to reflect differences in feeding behavior among predators (Therrien, 2005a,b; Therrien et al., 2005; Christiansen, 2007; Blanco et al., 2011; Jasinski, 2011).

Bite force estimation

Following the approach of Therrien (2005a), Zx/L values at the carnassial (P_4M_1 and M_1M_2 or post-M_1 in felids and *Crocuta*), where maximum bite force is theoretically achieved in carnivorans (Greaves, 1983, 1985), were used as a bite force proxy for each taxon. The Zx/L values of each taxon were compared to *P. leo*, providing a "relative bite force" estimate expressed as a percent (%) value of the bite force of the lion (Table 2).

To assess the accuracy of bite force estimates derived from mandibular force profiles, values were compared with bite force estimates derived from measurements of cross-sectional areas and lever arms of major jaw adductor muscles (the 'dry skull' method of Thomason, 1991) and empirical *in vivo* bite force measurements (Table 2). Because the bite force values from the various methods could only be compared if expressed in relative terms (i.e., relative to the lion bite force), we limited our search to studies that evaluated both the bite force of *P. leo* and of other taxa considered in our study in order to insure consistency of methodology and bite force estimates. Empirically measured bite forces, reported in absolute terms (i.e., Newtons), were expressed relative to Thomason's (1991) lion bite force estimates. Although an empirically-derived bite force for the lion would have been preferable, this

estimation method has been considered a reliable proxy in felids in the absence of empirical data (Sakomoto et al., 2010).

Statistical analyses

To compare the degree of hollowness of the various carnivoran mandibles, the CA/TA ratios at post-canine interdental gaps were compared for all specimens by performing a one-way ANOVA with post hoc tests for multiple comparison on samples where equal variance is not assumed using the software IBM SPSS Statistics 22.0.

RESULTS

Comparison of solid and hollow mandible models

Comparison via bivariate plots reveals that the solid and hollow mandible models follow similar trends but differ in absolute values, the magnitude of difference varying between species and as a function of the location along the mandible.

The solid mandible model generally overestimates the true biomechanical properties, as expressed by the hollow mandible model, of mandibular strength (Zx; Fig. 3) and mandibular force (Zx/L; Fig. 4). Posterior to P_3P_4, the solid mandible model overestimates Zx and Zx/L in canids and *Panthera leo* (by 10–31%), but significantly less so in *Crocuta* and *Neofelis* (<12%). At P_2P_3, the solid ellipse model overestimates Zx by approximately 30% in canids and *Crocuta*, 37% in *P. leo*, and 17% in *Neofelis*. (Because the distance from the articular condyle to P_2P_3 was only available for *Crocuta*, Zx/L values could only be calculated for this species and are overestimated by 29% by the solid ellipse model.) At the canine, the solid mandible model overestimates Zx and Zx/L in all carnivorans (by 25%-41%), except *Neofelis* where these values are slightly underestimated (by 4%).

In estimating the relative mandibular force (Zx/Zy), the solid ellipse model generally provides values close to those of the hollow mandible model (Fig. 5). Among canids, the Zx/Zy values produced by the two models are usually within 10% of each other, although the solid model consistently underestimates the values in the post-carnassial region. This underestimation of Zx/Zy values in the post-carnassial region is due to the fact that Zy values are overestimated to a greater extent (proportionally speaking) than Zx values by the solid model (see Table 1). In *Crocuta*, the Zx/Zy values produced by the two models are within 17% of each other and nearly identical at P_3P_4 and at the canine. In *Neofelis*, the Zx/Zy values produced by the two models are nearly identical along the entire tooth row, except behind the carnassial where the solid ellipse model underestimates the Zx/Zy value by 11%. The greatest

divergence is observed in *P. leo*, where the solid ellipse model overestimates Zx/Zy values by 5–20% along the entire tooth row, except behind the carnassial where it underestimates values by 25%.

CA/TA ratio

The hollowness of the mandible, expressed by the CA/TA ratio, varies along the mandible and between species (Fig. 6). All species have a nearly solid mandibular corpus at the canine (CA/TA ~95–99%) but differ in the posterior portion of the mandible. The mandibles of canids and *P. leo* are moderately solid (CA/TA ~73–86%), except in the postcarnassial region of *C. lupus* and at P_2P_3 in *P. leo* where they are more hollow (CA/TA ~63–64%). In contrast, the mandibles of *Crocuta* and *Neofelis* are generally far more solid (CA/TA ~86–92%), except at P_2P_3, where they are in the range observed among canids (70%-77%). These results indicate that the medullary cavity in the mandibles of *Crocuta* and *Neofelis* is much smaller than in other carnivorans, usually occupying only 8–14% of the mandibular cross-section contra 14%-37% in other carnivorans (see also Tseng and Binder, 2010). A statistical comparison of CA/TA values for all post-canine interdental gaps reveals that the mandibular corpus of *Crocuta* is significantly more solid than that of *C. lupus* and *P. leo* ($p<0.027$) and *C. dirus* ($p=0.097$), but similar to *Neofelis* ($p>0.957$).

Relative bite force estimates

Relative bite force estimates derived from the solid ellipse and hollow mandible models are generally consistent (within 4%) among most taxa, with the solid model usually underestimating bite force values produced by the hollow model (Fig. 7, Table 2). The reason why solid model produces lower bite force estimates when it generally overestimates Zx and Zx/L values is due to the fact that the lion mandible is more hollow at the carnassial than in other taxa, resulting in a greater discrepancy of Zx/L values between solid and hollow model in that reference taxon than in other taxa. The two models differ the most in *Crocuta*, where the solid mandible model underestimates relative bite force values by 10–14%. These results are largely consistent with Therrien's (2005a) bite force estimates based on the solid model (Fig. 7, Table 2), the slight incongruences most likely due to differences in the samples studied, i.e., mean of seven individuals in Therrien (2005a) versus mean of two individuals in this study. Interestingly, relative bite force estimates calculated anterior (at P_4M_1) and posterior (at M_1M_2 or post-M_1) to the carnassial differ by 4%-15%, except in *Crocuta* where the difference is much greater (15%-19%).

DISCUSSION

Our study demonstrates that mandibular force profiles are a reliable approach to document the biomechanical properties of carnivoran mandibles and, consequently, to infer the feeding behavior and bite force of extant and extinct taxa. Although the solid mandible model does not record the "true" biomechanical properties of the mandible, as represented by the hollow mandible model, the two approaches produce comparable results. While the solid ellipse model tends to overestimate mandibular strength (Zx) and mandibular force (Zx/L), it generally closely reflects relative mandibular force (Zx/Zy). Similar conclusions were reached by Biknevicius and Ruff (1992b) in their comparison of various approaches to calculate the second moment of area (I) of carnivoran mandibles. Although the difference between the solid and hollow mandible models is not always consistent between interdental gaps, which could raise concerns about the validity of the solid mandible model, this discrepancy is generally ≤20% (see Figs 3-5). While this discrepancy may appear large in relative terms, its absolute magnitude (0.04-0.12 for Zx/L and 0.4-0.8 for Zx/Zy) is so small that it often falls within the range of intraspecific variation (i.e., values between two similar-sized individuals of a given species can differ by as much as the solid model discrepancy, see Table 1). As such, the solid model discrepancy is minimal and does not alter interpretation of the results. Given the primary purpose of mandibular force profiles to infer feeding behavior, it is the relative pattern of change in biomechanical properties (primarily Zx/L and Zx/Zy ratios) along the mandible that is of relevance. The only instances where the actual value of a biomechanical property is used to infer feeding behavior is: 1) the Zx/Zy value at the canine (i.e., to infer the method of prey capture) and 2) the Zx/L values at the carnassial (i.e., to infer bite force) (see Therrien, 2005a). In the first case, the solid and hollow models are shown to produce nearly identical Zx/Zy values at the canine (ratio of the two models is ~1.0; see Fig. 5). In the second case, Zx/L values at the carnassial are shown to be nearly identical between the solid and hollow models (see *Accuracy of bite force estimates derived from mandibular force profiles* below). Consequently, the solid mandible model is a reliable approach to reconstruct feeding behavior. However, if one seeks to determine the exact values of the biomechanical properties of the mandible (e.g., to infer peak stress the mandible can withstand), the hollow mandible model should preferably be applied.

From an ecological and behavioral perspective, the general pattern of change in biomechanical properties along the mandible is consistent between solid and hollow models (Figs. 3–5), resulting in identical feeding behavior interpretations for the carnivorans studied. Furthermore, the fact that the magnitude of change in biomechanical properties exceeds the

aforementioned solid-hollow model discrepancy and intraspecific variation confirms the validity of mandibular force profile analysis for feeding behavior reconstructions. The much lower Zx/L values at the canine than at the carnassial seen in canids and *Crocuta* reflect their pack hunting behavior, where individuals deliver numerous shallow canine bites to weaken prey (e.g., Kruuk, 1972; Ewer, 1973; Biknevicius and Ruff, 1992a; Therrien, 2005a). The higher Zx/L values at the canine and steeper increase in Zx/L values along the tooth row observed in the extinct *C. dirus* presumably reflect mandibular adaptations to subdue large Pleistocene herbivores (Therrien, 2005a; see also Anyonge and Baker, 2006). In contrast, the high Zx/L values at the canine relative to at the carnassial observed in felids reflect the powerful, canine killing bite these solitary hunters deliver to subdue prey (Kruuk and Turner, 1967; Schaller, 1972; Ewer, 1973; Therrien, 2005a).

Mandibular force profiles provide insight into the bone-cracking abilities of carnivorans (see Therrien, 2005a). While pre-carnassial (i.e., P_4M_1 and P_3P_4) Zx/Zy values remain constant in felids and canids, reflecting the fact that this region of the mandible is used for slicing flesh exclusively, they increase posteriorly in *Crocuta*. This increase in Zx/Zy values over the pre-carnassial corpus reflects a species that cracks bone with the premolars (Rensberger, 1995; Van Valkenburgh, 1996). By contrast, canids crush bones with their post-carnassial molars (M_1-M_3; Ewer, 1973) and, in these species, the increase in Zx/Zy values occurs posterior to M_1. The more anteriorly situated bone-processing location in hyaenids allows them to break larger bones but requires relatively larger bite forces due to the reduced mechanical advantage induced by cracking bones at a greater distance from the jaw joint (Greaves, 1985) and deeper mandibular corpora (i.e., posteriorly- increasing Zx/Zy values) to sustain stresses associated with this behavior (Biknevicius and Ruff, 1992a). The post-carnassial Zx/Zy values of canids, including the extinct *C. dirus*, are lower than those of *Crocuta*, as originally noted by Therrien (2005a), which indicate poorer adaptations for bone processing. Although both canids have less cortical bone in their mandibular cross-section than hyaenids (Fig. 6), the post-carnassial mandibular corpus of *C. dirus* is characterized by slightly thicker (9-13%) cortical bone than that of *C. lupus* (Fig. 6), resulting in greater mandibular bending strength (Zx) values in the extinct canid, approaching values observed in *Crocuta* (Fig. 3). Nevertheless, the lower Zx/Zy values produced by hollow mandible models confirm that dire wolves were not as adept bone crushers as modern gray wolves and clearly lacked the adaptations for osteophagy of hyaenids (Van Valkenburgh et Koepfli, 1993; Therrien, 2005a; Anyonge and Baker, 2006; contra Meehan and Martin, 2003). Indeed, extant canids are considered unspecialized for osteophagy (Biknevicius and Ruff, 1992a) and tend

to crush bones rather than crack them like hyaenids (Werdelin, 1989). Despite having a mandible characterized by a very thick layer of cortical bone like that of *Crocuta*, *Neofelis* does not display any biomechanical mandibular adaptations associated with osteophagy (i.e., the Zx/Zy profile remains constant over the cheek teeth, indicative of a slicing function). Furthermore its highly specialized dentition, characterized by a blade-like carnassial, absence of postcarnassial teeth, and narrowed premolars, is indicative of a hypercarnivorous diet without bone cracking abilities (Holliday and Steppan, 2004). Thus the thickened cortical bone layer of this felid is not an adaptation to withstand bending stresses associated with bone cracking. *Neofelis* is known for hunting prey both smaller (e.g., small primates, birds) and far larger than itself (e.g., large primates, deer, wild boars), which it dispatches with a powerful bite to the back of the neck (see Banks, 1949; Prater, 1971; Payne et al., 1985; Rabinowitz et al. 1987; Grassman et al., 2005; Chiang 2007). Thus the greater cortical bone thickness of the mandibular corpus in *Neofelis* may be an adaptation to deliver powerful bites to capture large prey. Interestingly, this mandibular condition is also observed in sabertoothed predators (Akersten, 1985; Biknevicius and Van Valkenburgh, 1996; McHenry et al., 2007), adding to the list of convergences between *Neofelis* and these extinct predators (Therrien, 2005b; Christiansen, 2005, 2008).

Although the thickened mandibular corpus of *Crocuta* certainly offers a biomechanical advantage for bone cracking (see Biknevicius and Ruff, 1992a), the question of whether this condition represents an adaptation for osteophagy rather than a phylogenetic signal has yet to be investigated. The facts that early hyaenids were civet-like insectivores/omnivores and that craniodental features indicative of bone-cracking abilities did not evolve until later (e.g., Werdelin and Solounias, 1996; Turner et al., 2008) suggests that thickened mandibular corpora may be an adaptation for durophagy in that clade. However, resolving this question would require the study of a vast array of carnivoran species across a broad taxonomic spectrum and would far exceed the scope of the current manuscript. Nevertheless, the fact that both *Neofelis* and the sabretooth *Smilodon* possess thicker mandibular corpora indicates that this condition also occurs in non-osteophagous taxa. As such, the presence of a thickened mandibular corpus may not be exclusively an adaptation for osteophagy but rather an adaptation to sustain greater stresses associated with powerful bites, be it for durophagy or for subduing large prey. Interestingly, a thickened mandibular corpus evolved independently in some aquatic vertebrates as an adaptation for buoyancy or bottom feeding (Domning and Debuffrenil, 1991; Houssaye, 2009; Jones et al, 2013) and not for delivering powerful bites.

Accuracy of bite force estimates derived from mandibular force profiles

The hollow mandible model should theoretically provide more accurate bite force estimates than the solid ellipse model because it takes into consideration cortical bone distribution and thickness in the mandibular cross-section. Comparison of the two models, however, reveals that relative bite force estimates are usually close (within 4% of each other), with the greatest divergence (10%-14%) found in *Crocuta*. This divergence is due to the significantly greater thickness of cortical bone in hyaenid mandibles (CA/TA ~90%) relative to other carnivorans (CA/TA ~60%-85%). Thus the solid mandible models produce bite force estimates that are nearly identical to the hollow mandible models, except in taxa with a thick cortical bone layer in the mandibular corpus.

Large differences exist between bite force estimates derived from the hollow mandible model and those obtained from the dimension of the jaw adductor musculature (Fig. 7, Table 2). The least extreme differences are observed in *N. nebulosa*, where the bite force estimates derived from hollow mandible models are generally within 17% (depending on the landmark being considered) of those based on jaw musculature dimension. In canids, the hollow mandible model provides bite force estimates that are 7%–27% higher than those based on jaw adductor musculature. The greatest differences are observed in *Crocuta*, where the hollow mandible model provides estimates that are 42%–70% higher than those based on jaw adductor musculature.

Ultimately, true assessment of the accuracy of bite force estimates produced by mandibular force profiles requires comparison with experimentally-determined bite force values (i.e., recorded in live subjects). Despite a plethora of bite force values presented in documentaries and blogs, experimentally-determined bite force values have been published for few mammal species (Thomason et al., 1990; Dessem and Druzinsky, 1992; Ström and Holm, 1992; Binder and Van Valkenburgh, 2000; Ellis et al., 2008). Of relevance to our study, the highest recorded bite force for *Crocuta* approaches 4500 N (Binder and Van Valkenburgh, 2000:fig. 3a) and preliminary attempts to empirically determine the bite force of *Canis lupus* (Thomas et al., 2005) reveal a bite force of approximately 2000 N (Nancy L. Denton, Purdue University, personal communication). Comparison reveals that mandibular force profiles consistently produce bite force estimates that are far closer to the empirically-measured bite force (accuracy to within 4%-15% for the hollow model and 10%-25% for the solid model) than those produced by the jaw musculature method (11%-16% lower in *C. lupus* and 57%-66% lower in *Crocuta*) (Fig. 7, Table 2). Even after application of the correction factor for the disparity between dry skull and *in vivo* bite force (Thomason, 1991;

Sakomoto et al., 2010), absolute bite force estimates produced by the jaw musculature method are still 23%-52% lower than empirical bite forces for *Crocuta* (also noted by Tseng and Binder, 2010), but are slightly closer for *C. lupus* (ranging from 15% lower to 39% higher than empirical values) (Fig. 7, Table 2).

These results support the long-held suspicion that the jaw musculature method greatly underestimates bite force (see Therrien, 2005a; Ellis et al., 2008; Davis et al., 2010), although the congruence between empirically-determined and hollow model-derived bite force values expressed relative to *P. leo* suggests that the jaw musculature method might produce accurate bite force estimates for this felid (see Sakomoto et al., 2010). The poorer performance of the jaw musculature method has been ascribed to a variety of issues, such as the facts that the method does not account for interspecific variation in jaw muscle pennation, assumes that muscle cross-sectional area and lever arm length correlate directly with bite force, or that the mandible is considered only in two dimensions, which overestimates the cross-sectional area of the masseter and pterygoid muscles and underestimates the cross-sectional area of the temporalis muscle in many carnivorans (Wroe et al., 2005; Ellis et al., 2008; Davis et al., 2010; Tseng and Binder, 2010). Thus mandibular force profiles, particularly the hollow mandible model, are a more accurate and far simpler method to estimate bite force than the jaw musculature method.

Given the greater accuracy of bite force estimates derived from mandibular force profiles, this method can be used to infer the bite force of the extinct *C. dirus* and the elusive *Neofelis*. Previous studies have shown that *C. dirus* was similar to *C. lupus* in terms of feeding behavior but, due to its overall larger size and robustness, could deliver a stronger bite (see Therrien, 2005a; Anyonge and Baker, 2006; Meloro et al., 2015). Supporting this view, the hollow mandible model indicates *C. dirus* had a bite force that was 11%-59% stronger than that of *C. lupus* (8%–25% when expressed relative to *P. leo*), values paralleled by the jaw musculature method (Wroe et al., 2005). This hollow mandible model thus confirms that *C. dirus* was capable of a very powerful bite, presumably an adaptation to kill large Pleistocene prey. In comparison, the estimated bite force of *Neofelis* is approximately 20% that of *P. leo*, values that are generally lower than estimates produced by the jaw adductor musculature method, except for one study (Fig. 7, Table 2). It is unclear why bite force estimates based on the jaw musculature method are generally higher in this instance, but it does not seem to be related to the study of larger individuals as both methods employed individuals of similar size (compare Therrien [2005a:table 1] with Wroe et al. [2005:table 1]).

Implications for the calibration of finite-element analysis (FEA) models

Over the past two decades, FEA has been used extensively to investigate the relationship between form and function in extant and extinct animals (for a review, see Fastnacht et al., 2002; Rayfield, 2007; and Cunningham et al., 2014). Although this non-destructive approach has gained in popularity, it remains anchored in numerous assumptions, including some about cranial and muscle architecture and the amount of force generated by the jaw musculature (Fastnacht et al., 2002; Bright, 2014). While muscle architecture can be inferred from muscle scars and dissection of extant relatives, the amount of force muscles can generate is often based, in the absence of empirically-determined values, on bite force estimates derived from jaw musculature reconstructions (e.g., Wroe et al., 2007; McHenry et al., 2007; Wroe, 2008; Slater et al., 2009). As noted above, bite force estimates derived from such methods tend to dramatically underestimate true bite force in mammalian predators. As such, while FEA can be used to document and compare stress and load distributions in skulls of different morphology, use of this method to infer the bite force generated by a predator or to infer stress distribution during "typical bite" ought to be done with caution (Bright, 2014). While other approaches have been developed to produce more accurate bite force estimates in carnivorans (e.g., Wroe et al., 2008; Tseng and Wang, 2010; Tseng and Binder, 2010; Slater et al., 2010), mandibular force profiles may represent a simpler alternative method to obtain accurate bite force values (after converting relative bite force estimates to absolute values) with which FEA models can be calibrated.

CONCLUSION

The mandibular force profile approach provides a simple and widely applicable method to investigate the feeding behaviors and bite force of extant and extinct predators. Although the method is theoretically sensitive to the distribution of cortical bone within the mandibular corpus, comparison of results derived from the precise quantification of bone distribution via computed tomography (i.e., hollow mandible model) with those derived from external mandibular dimensions assuming a solid mandible (i.e., solid mandible model) reveals that the two models are highly congruent. The solid mandible model generally overestimates biomechanical properties relative to the hollow mandible model, but the overall pattern of change along the jaw is accurately represented. Furthermore, bite force estimates produced by the two models are highly similar to each other and to empirically-determined bite force, except for the spotted hyaena *Crocuta* due to the greater cortical bone thickness in the mandibular corpus of this osteophagous taxon. Consequently, reconstruction of the

feeding behaviour and bite force for most carnivorans can be achieved with the solid ellipse model without the need for time-consuming, often limited access, and costly computed tomography. Only when dealing with a taxon that possesses thicker cortical bone within its mandibular corpus (e.g., hyaenids, sabertooths) will the solid model slightly underestimate the bite force of the animal. Thus, computed tomography may help provide more accurate bite force estimates for these taxa by permitting documentation of the internal distribution of cortical bone in the mandibular corpus.

Finally, mandibular force profiles, based on either the solid or hollow models, are shown to produce more accurate bite force estimates than those derived from jaw muscle architecture measurements on dry skulls. This discrepancy has important implications for the use of FEA, as this method often uses bite force estimates inferred from muscle architecture measurements to calibrate virtual models of extant an extinct taxa. Use of incorrect bite force values may affect the validity of FEA models, especially as it relates to predicting the bite force of extinct taxa and documenting stress distribution during bite. Mandibular force profiles may thus provide an alternative method to obtain more accurate bite force estimates for finite-element analysis in the absence of actual bite force values. Furthermore, given that the feeding behaviors reconstructed from mandibular force profiles are generally consistent with those obtained from the FEA studies (e.g., Tseng and Binder, 2010), mandibular force profile analysis has great potential for elucidating the ecology of extinct predators known from limited fossilized remains.

ACKNOWLEDGMENTS

We wish to thank Bruno Frohlich (Dept. of Anthropology, USNM) for assistance with CT scanning, Linda Gordon (Dept. of Vertebrate Zoology – Mammals Division, USNM) and Robert Purdy and Michael Brett-Surman (Dept. of Paleobiology - Vertebrate Paleontology Division, USNM) for access to specimens in their care. We are indebted to Nancy L. Denton (Purdue Polytechnic Institute, Purdue University) for sharing unpublished bite force measurements in gray wolves and to Rachel Frigot (Johns Hopkins University – School of Medicine) for providing missing length measurements on two specimens. We also wish to thank Susan Virtue for her assistance in compiling tables and formatting the manuscript. Finally, we are grateful to Blaire Van Valkenburgh and one anonymous reviewer for their thorough review that helped improve the manuscript.

COMPETING INTERESTS

The authors declare no competing or financial interests.

AUTHOR CONTRIBUTIONS

FT conceived the study. FT and AQ conducted the analyses. All authors assessed the results and wrote the manuscript.

FUNDING

This work was partially supported by a Natural Sciences and Engineering Research Council (NSERC) Discovery Grant (327513-2009 to DKZ).

REFERENCES

Akersten, (1985). Canine function in *Smilodon*. *Contributions in Science, Natural History Museum of Los Angeles County* **356**, 1-22.

Anyonge, W. and Baker, A. (2006). Craniofacial morphology and feeding behavior in *Canis dirus*, the extinct Pleistocene dire wolf. *Journal of Zoology* **269**, 309-316.

Banks, E. (1949). *Bornean mammals.*Kuching: Kuching Press.

Biewener, A.A. (1992). Overview of structural mechanics. In *Biomechanics, Structures and Systems: a Practical Approach. The Practical Approach Series* (ed. A.A. Biewener), pp. 1-20. Oxford: Oxford University Press.

Biknevicius, A. and Ruff, C.B. (1992a). The structure of the mandibular corpus and its relationship to feeding behaviours in extant carnivorans. *Journal of Zoology* **228**, 479-507.

Biknevicius, A. and Ruff, C.B. (1992b). Use of biplanar radiographs for estimating cross-sectional geometric properties of mandibles. *The Anatomical Record* **232**, 157-163.

Biknevicius, A. and Van Valkenburgh, B.A. (1996). Design for killing: craniodental adaptations of predators. In *Carnivore Behavior, Ecology, and Evolution, Volume 2* (ed. J.L. Gittleman), pp. 393-428. Ithaca: Cornell University Press.

Binder, W.J. and Van Valkenburgh, B. (2000). Development of bite strength and feeding behaviour in juvenile spotted hyenas (*Crocuta crocuta*). *Journal of Zoology* **252**, 273-283.

Blanco, R.E., Jones, W.W. and Grinspan, G.A. (2011). Fossil marsupial predators of South America (Marsupialia, Borhyaenoidea): bite mechanics and palaeobiological implications. *Alcheringa* **35**, 377-387.

Bright, J.A. (2014). A review of paleontological finite element models and their validity. *Journal of Paleontology* **88**, 760-769.

Christiansen, P. (2007). Evolutionary implications of bite mechanics and feeding ecology in bears. *Journal of Zoology* **272**, 423-443.

Christiansen, P. (2008). Evolution of skull and mandible shape in cats (Carnivora: Felidae). *PLoS ONE* **7**, e2807. doi:10.1371/journal.pone.0002807.

Christiansen, P. and Adolfssen, J.S. (2005). Bite forces, canine strength and skull allometry in carnivores (Mammalia, Carnivora). *Journal of Zoology* **266**, 133-151.

Christiansen, P. and Wroe, S. (2007). Bite forces and evolutionary adaptations to feeding ecology in carnivores. *Ecology* **88**, 347-358.

Cunningham, J.A., Rahman, I.A., Lautenschlager, S., Rayfield, E.J., and Donoghue, C.J. (2014). A virtual world of paleontology. *Trends in Ecology & Evolution.* **29**, 347-357

Davis, J. Santana, S. Dumont E. and Gross, I. (2010). Predicting bite force in mammals: two-dimensional versus three-dimensional models. *The Journal of Experimental Biology* **213**, 1844-1851.

Dessem, D. and Druzinsky, R.E. (1992). Jaw-muscle activity in ferrets (*Mustela putorius furo*). *Journal of Morphology.* **213**, 275-286.

Domning, D.P. and Debuffrenil, V. (1991). Hydrostasis in the Sirenia: quantitative data and functional interpretations. *Marine Mammal Science* **7**: 331-368.

Ellis, J.L. Thomason, J.J. Kebreab, E. and France, J. (2008). Calibration of estimated biting forces in domestic canids: comparison of post-mortem and *in vivo* measurements. *Journal of Anatomy* **212**, 769-780.

Ewer, R.F. (1973). The Carnivores. Ithaca: Cornell University Press.

Fastnacht, M., Hess, N., Frey, E. and Weiser, H.-P. (2002). Finite element analysis in vertebrate palaeontology. *Senckenbergiana lethaea* **82**, 195-206.

Figueirido, B., Tseng, Z.J., Serramp-Alarcon, F.J., Martin-Serra, A. and Pastor, J.F. (2014). Three-dimensional computer simulations of feeding behaviour in red and giant pandas relate skull biomechanics with dietary niche partitioning. *Biology Letters* **10**, 20140196.http://dx.doi.org/10.1098/rsbl.2014.0196.

Grassman, L.I. Jr., Tewes, M.E. Sukvy, N.J. and Kreetiyutanont, K. (2005). Ecology of three sympatric fields in a mixed evergreen forest in north-central Thailand. *Journal of Mammalogy* **86**, 29-38.

Greaves, W. (1983). A functional analysis of carnassial biting. *Biological Journal of the Linnean Society* **20**, 353-363.

Greaves, W. (1985). The generalized carnivore jaw. *Zoological Journal of the Linnean Society* **85**, 267-274.

Holiday, J.A. and Steppan, S.J. (2004). Evolution of hypercarnivory: the effect of specialization on morphological and taxonomic diversity. *Paleobiology* **30**, 108-128.

Houssaye, A. (2009). "Pachyostosis" in aquatic amniotes: a review. *Integrative Zoology* **4**: 325-340.

Jasinski, S. (2011). Biomechanical modeling of *Coelophysis bauri*: possible feeding methods and behavior of a Late Triassic theropod. *New Mexico Museum of Natural History and Science Bulletin* **53**, 195-201.

Jones, K.E., Ruff, C.B. and Goswami, A. (2013). Morphology and biomechanics of the pinniped jaw: mandibular evolution without mastication. *The Anatomical Record* **296**, 1049-1063.

Kruuk, H. (1967). Comparative notes on predation by lion, leopard, cheetah and wild dog in the Serengeti area, East Africa. *Mammalia* **31**, 1-27.

Kruuk, H. (1972). The Spotted Hyena. Chicago: University of Chicago Press.

Kruuk, H., and Turner, M. (1967). Comparative notes on predation by lion, leopard, cheetah and wild dog in the Serengeti area, East Africa. *Mammalia* 1-23.

Lanyon, L.E. and Rubin, C.T. (1985). Functional adaptation in skeletal structures. In *Functional Vertebrate Morphology* (ed. M. Hildebrand, D.M. Bramble, K.F. Liem and D.B. Wake), pp. 1-25. Cambridge: Harvard University Press.

McHenry, C.R. Wroe, S. Clausen, P.D. Moreno, K. and Cunningham, E. (2007). Supermodeled sabercat, predatory behavior in *Smilodon fatalis* revealed by high-resolution 3D computer simulation. *Proceedings of the National Academy of Sciences* **104**, 16010-16015.

Meehan, T.J. and Martin, L.D. (2003). Extinction and re-evolution of similar adaptive types (ecomorphs) in Cenozoic North American ungulates and carnivores reflect van der Hammen's cycles. *Naturwissenschaften* **90**, 131-135.

Meers, M.B. (2002). Maximum bite force and prey size of *Tyrannosaurus rex* and their relationships to the inference of feeding behavior. *Historical Biology* **16**, 1-12.

Meloro, C., Hudson, A. and Rook, L. (2015). Feeding habits of extant and fossil canids as determined by their skull geometry. *Journal of Zoology* **295**, 178-188.

Organ, J.M., Ruff, C.B., Teaford, M.F. and Nisbett, R.A. (2006). Do mandibular cross-sectional properties and dental microwear give similar dietary signals? *American Journal of Physical Anthropology* **130**, 501-507.

Payne, J., Francis, C.M. and Phillips, K. (1985). *A Field Guide to the Mammals of Borneo. Malaysia:Sabah Society.*

Prater, S.H. (1971). *The Book of Indian Mammals.* 3rd Edn. Bombay: Bombay Natural History Society.

Rabinowitz A.R., Andau, P. and Chai, P.P.K. (1987). The clouded leopard in Malaysian Borneo. *Oryx* **22**, 107-111.

Rayfield, E.J. (2007). Finite element analysis and understanding the biomechanics and evolution of living and fossil organisms. *Annual Review of Earth and Planetary Sciences* **35**, 541-576.

Ridgely, R, and Witmer, L.M. (2006). Dead on arrival: optimizing CT data acquisition of fossils using modern hospital CT scanners. Journal of Vertebrate Paleontology Abstract with Programs **26**, 115A.

Rensberger, J.M. (1995). Determination of stresses in mammalian dental enamel and their relevance to the interpretation of feeding bahaviors in extinct taxa. In *Functional Morphology in Vertebrate Paleontology* (ed. J. Thomason), pp. 151-172. Cambridge: Cambridge University Press.

Sakamoto, M. Lloyd, G.T. and Benton, M.J. (2010). Phylogenetically structured variance in felid bite force: the role of phylogeny in the evolution of biting performance. *Journal of Evolutionary Biology* **23**, 463-478.

Schaller, G.B. (1972). *The Serengeti Lion.* Chicago: University of Chicago Press.

Slater, G.J., Dumont, E.R., and Van Valkenburgh, B. (2009) Implications of predatory specialization for cranial form and function in canids. *Journal of Zoology* **278**, 181-188.

Slater, G.J., Figueirido, B., Louis, L., Yang, P. and Van Valkenburgh, B. (2010). Biomechanical consequences of rapid evolution in the polar bear lineage. *PLoS ONE* **5**, e13870.doi:10.1371/journal.pone.0013870.

Ström, D. and Holm, S. (1992). Bite force development, metabolic and circulatory response to electrical stimulation in the canine and porcine masseter muscles. *Archives of Oral Biology* **37**, 997-1006.

Therrien, F. (2005a). Mandibular force profiles of extant carnivorans and implications for the feeding behaviour of extinct predators. *Journal of Zoology* **267**, 249-270.

Therrien, F. (2005b). Feeding behaviour and bite force of sabretoothed predators. *Zoological Journal of the Linnean Society* **145**, 393-426.

Therrien, F. Henderson, D.M. and Ruff, C.B. (2005). Bite me: biomechanical models of theropod mandibles and implications for feeding behavior. In *The Carnivorous Dinosaurs* (ed. K. Carpenter), pp. 179-237. Bloomington: Indiana University Press.

Thomas, S.L., Shadd, A., Denton, N.L. and French, R.M. (2005). Design validation and testing of wolf bite meter. *American Society for Engineering Education IL/IN Sectional Conference*, 1-7.

Thomason, J.J., Russell, M. and Morgeli, M. (1990). Forces of biting, body size and masticatory muscle tension in the opossum *Didelphis virginiana*. *Canadian Journal of Zoology* **68**, 318-324.

Thomason, J.J. (1991). Cranial strength in relation to estimated biting forces in some mammals. *Canadian Journal of Zoology* **69**, 2326-2333.

Timoshenko, S.P. and Gere, J.M. (1972). Mechanics of materials. New York: Van Nostrand Reinhold.

Tseng, Z.J. (2013). Testing adaptive hypotheses of convergence with functional landscapes: a case study of bone-cracking hypercarnivores. PLoS ONE 8, e65305. doi:10.1371/journal.pone.0065305

Tseng, Z.J. and Binder, W.J. (2010). Mandibular biomechanics of *Crocuta crocuta, Canis lupus*, and the late Miocene *Dinocrocuta gigantea* (Carnivora, Mammalia). *Zoological Journal of the Linnean Society* **158**, 683-696.

Tseng, Z.J. and Wang, X. (2010). Cranial functional morphology of fossil dogs and adaptation for durophagy in *Borophagus* and *Epicyon* (Carnivora, Mammalia). *Journal of Morphology* **271**, 1386-1398.

Tseng, Z.J., Anton, M. and Salesa, M.J. (2011).The evolution of the bone-cracking model in carnivorans: cranial functional morphology of the Plio-Pleistocene cursorial hyaenid *Chasmaporthetes lunensis* (Mammalia: Carnivora). *Paleobiology* **37**, 140-156.

Turner, A, Antón, M. and Werdelin, L. (2008). Taxonomy and evolutionary patterns in the fossil Hyaenidae of Europe. *Geobios* **41**, 677-687.

Van Valkenburgh, B. (1996). Feeding behavior in free-ranging, large African carnivores. *Journal of Mammalogy* 240-254.

Van Valkenburgh, B. (2007). Déjà vu: the evolution of feeding morphologies in the Carnivora. *Integrative and Comparative Biology*. **47**, 147-163.

Van Valkeburgh, B. and Koepfli, K.-P. (1993). Cranial and dental adaptations to predation in canids. In *Mammals as predators* (ed. N. Dunston & J.L. Gorman), pp.15-37. Oxford: Oxford University Press.

Wainwright, S.A., Biggs, W.D., Currey, J.D. and Gosline, J.M. (1982). Mechanical design in organisms. Princeton: Princeton University Press.

Werdelin, L. (1989). Constraint and adaptation in the bone-cracking canid *Osteoborus* (Mammalia: Canidae). *Paleobiology* 387-401.

Werdelin, L. and Solounias, N. (1996). The evolutionary history of hyenas in Europe and western Asia during the Miocene. In Later Neogene European biotic evolution and stratigraphic correlation (ed. R.L. Bernor, V. Fahlbusch & S. Rietschel), pp. 290-306. New York: Columbia University Press.

Wroe, S. and Milne, N. (2007). Convergence and remarkably consistent constraint in the evolution of carnivore skull shape. *Evolution* **61**, 1251-1260.

Wroe, S., McHenry, C. and Thomason, J. (2005). Bite club: comparative bite force in big biting mammals and the prediction of predatory behaviour in fossil taxa. *Proceedings of the Royal Society B* **272**, 619-625.

Wroe, S., Chamoli, U., Parr, W.C.H., Clausen, P., Ridgely, R., and Witmer, L. (2013). Comparative biomechanical modeling of metatherian and placental saber-tooths: a different kind of bite for an extreme pouched predator. *PLoS ONE* **8**, e66888. doi:10.1371/journal.pone.0066888.

Figures

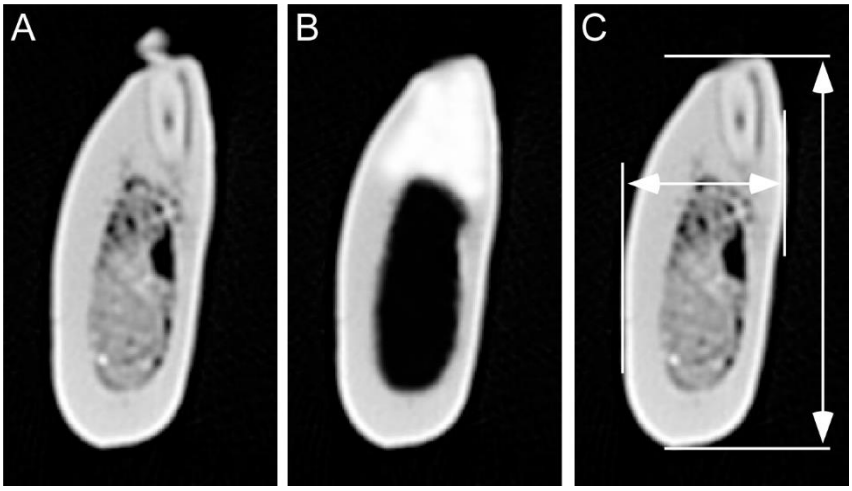

Figure 1. Use of computed tomographic (CT) scans to calculate the biomechanical properties of carnivoran mandibles. A) Raw CT slice. B) Alteration of CT slice to remove cancellous bone/tooth crown and fill cortical bone/tooth alveolus to determine biomechanical properties following the hollow mandible model. C) External linear measurements of mandibular corpus used to determine biomechanical properties following the solid mandible model. The CT slice illustrated is the M_2M_3 interdental gap of *Canis dirus* (USNM 8305).

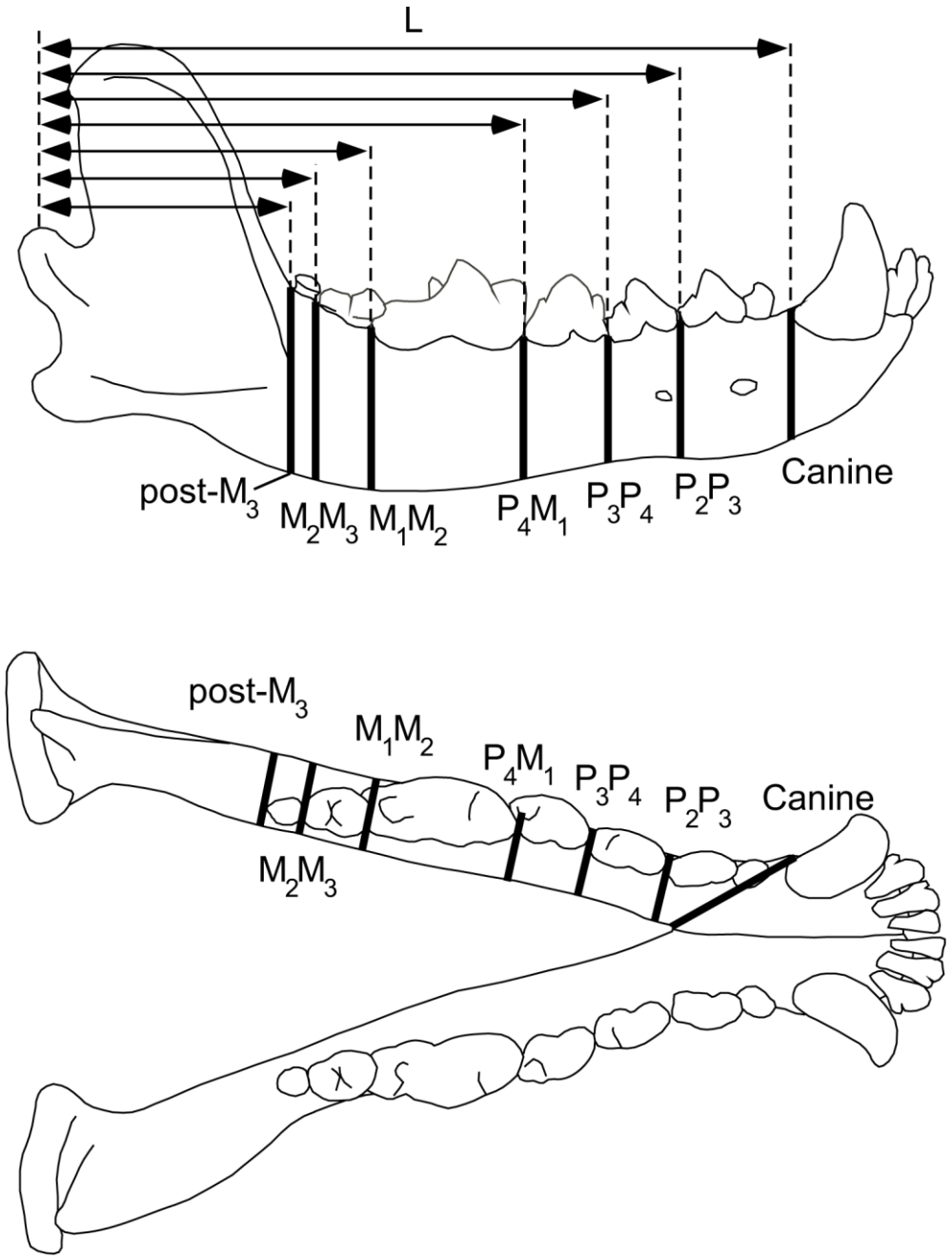

Figure 2. Orientation of CT slices taken at interdental gaps along the mandible. The mandibular ramus was oriented in life position and CT scans taken at each interdental gap in the coronal plane, perpendicular to the central axis of the mandible. At the canine, CT scans were taken diagonally from the lingual aspect of the symphysis through the posterior margin of the canine alveolus. Distance of each interdental gap to the articular condyle (L) was also measured (double-headed arrows).

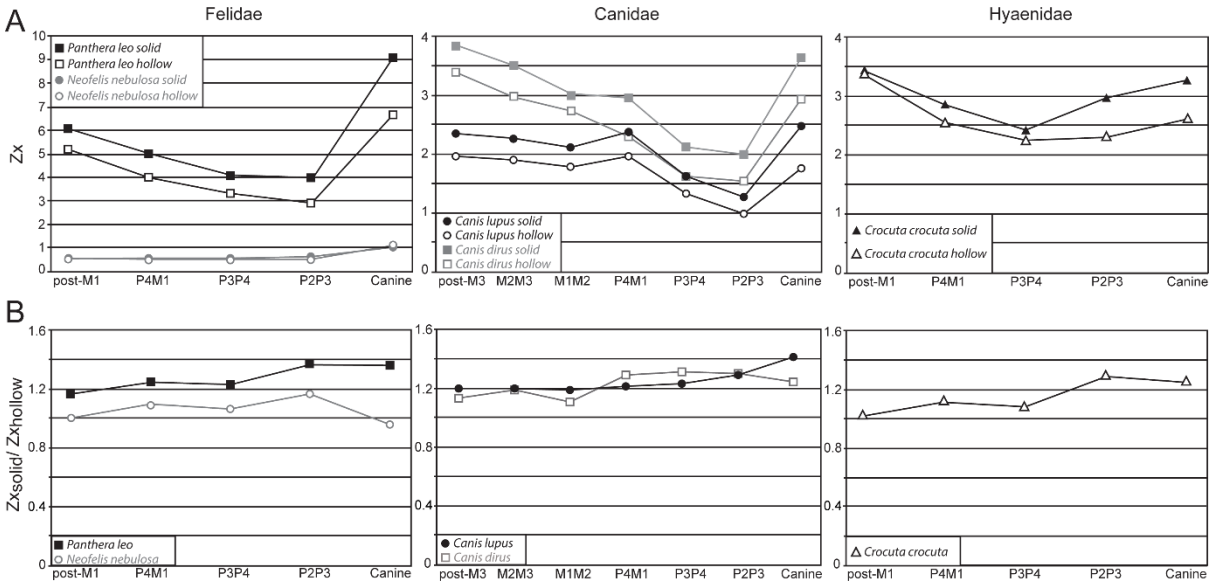

Figure 3. Comparison of Zx values obtained from the solid and hollow mandible models for studied carnivorans. A) Profiles of Zx values along the mandible. The pattern of change in Zx along the mandible is nearly identical in the two models, but the values for the solid model slightly exceed those for the hollow model. B) Ratios of Zx values obtained from the solid and hollow mandible models. The solid model slightly overestimates Zx values produced by the hollow model, generally by ~20% (i.e., ratio close to 1.2), except in *Neofelis* and *Crocuta* where Zx values are more similar (i.e., ratio closer to 1.0). The solid model overestimates Zx at the canine in all carnivorans except in *Neofelis*, where it is slightly underestimated.

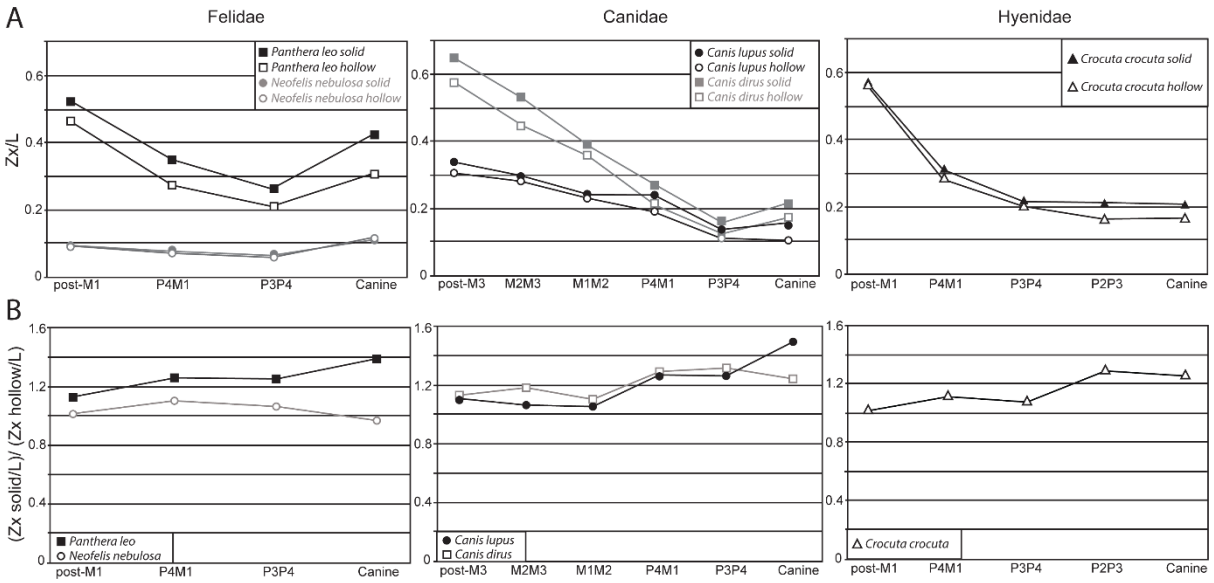

Figure 4. Comparison of Zx/L values obtained from the solid and hollow mandible models for studied carnivorans. A) Profile of Zx/L values along the mandible. The pattern of change in Zx/L along the mandible is nearly identical in the two models, but the values for the solid model slightly exceed those for the hollow model. B) Ratios of Zx/L values obtained from the solid and hollow mandible models. The solid model slightly overestimates Zx/L values produced by the hollow model, generally by ~10-30% (i.e., ratio varying between 1.1-1.3), except in *Neofelis* and *Crocuta* where Zx/L values are more similar (i.e., ratio closer to 1.0). The solid mandible model overestimates Zx/L at the canine in all carnivorans except in *Neofelis*, where it is slightly underestimated.

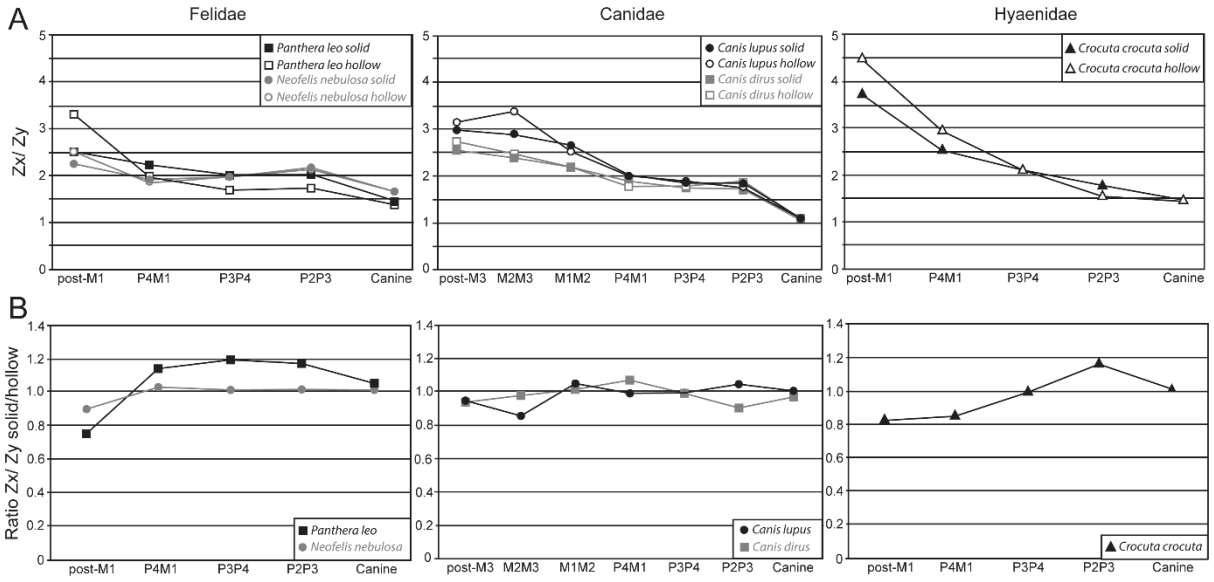

Figure 5. Comparison of Zx/Zy values obtained from the solid and hollow mandible models for studied carnivorans. A) Profile of Zx/L values along the mandible. The pattern of change in Zx/Zy along the mandible is nearly identical in the two models. B) Ratios Zx/Zy values obtained from the solid and hollow mandible models. The solid ellipse model generally provides values close to those of the hollow mandible model. Among canids, the two models are usually within 10% of each other, although the solid model consistently underestimates the values in the post-carnassial region. In *Crocuta*, the two models are within 17% of each other and are nearly identical at P_3P_4 and at the canine. In *Neofelis*, the two models are nearly identical along the entire tooth row, except behind the carnassial where the solid ellipse model underestimates Zx/Zy by 11%. In *Panthera leo*, the solid ellipse model overestimates Zx/Zy values by 5–20% along the entire tooth row, except behind the carnassial where it underestimates values by 25%.

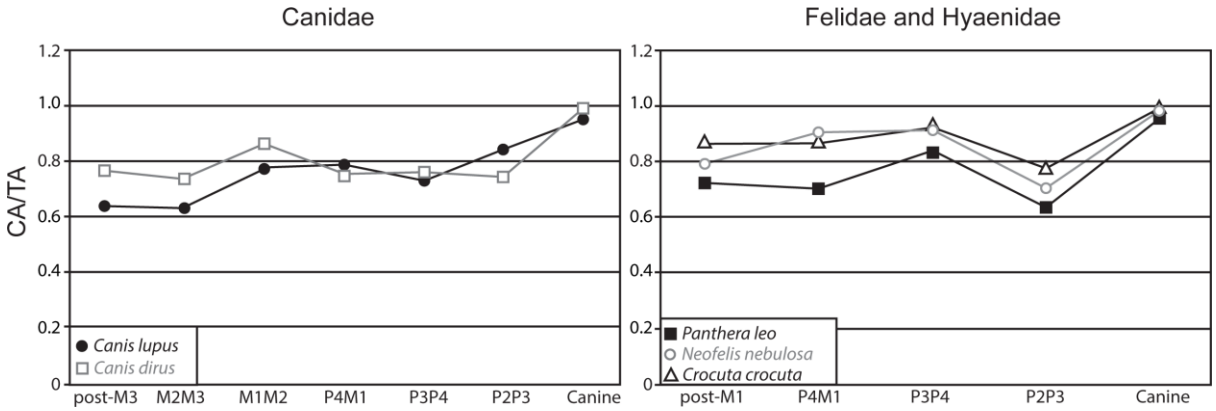

Figure 6. Comparison of CA/TA values for studied carnivorans. The mandibles of canids and *P. leo* are moderately solid (73%–86%), except in the postcarnassial region of *C. lupus* and at P_2P_3 in *P. leo* where they are more hollow (~63%). The mandibles of *Crocuta* and *Neofelis* are generally far more solid (86–92%), except at P_2P_3, where they are in the range observed among canids (70%-77%). All species have nearly solid mandibles at the canine (95–99%).

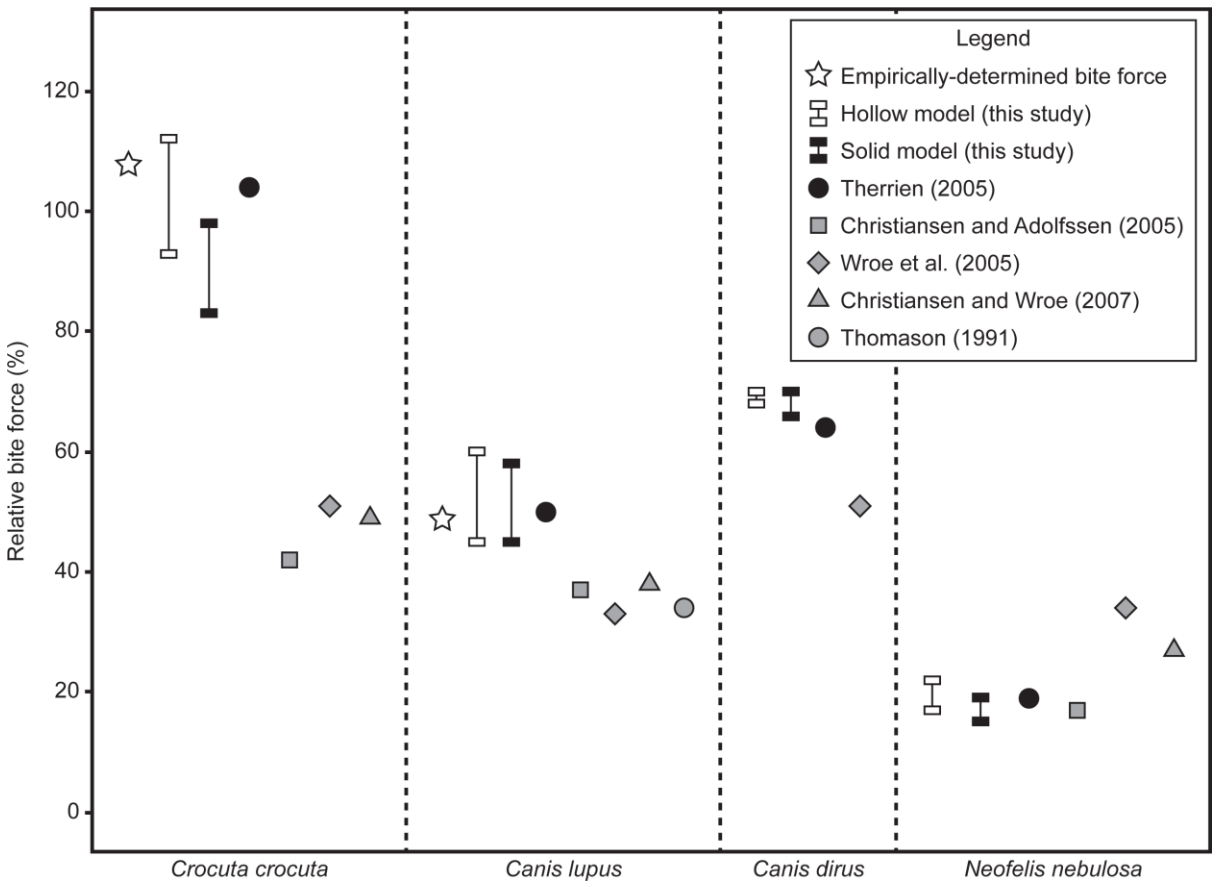

Figure 7. Comparison of bite force estimates obtained from various methods. Each bite force estimate is reported relative to the bite force value of *Panthera leo* obtained by the same estimation method. Estimates derived from mandibular force profiles (solid and hollow model) are generally higher and closer to empirically-determined bite force (star) than those derived using Thomason's (1991) jaw musculature method (gray symbols). Only in *Neofelis* are bite force estimates derived from mandibular force profiles lower or equal to those derived from the jaw musculature method.

Table 1. Mandibular dimensions and biomechanical properties of carnivorans.

Specimen/Interdental Gap	Depth (cm)	Width (cm)	L (cm)	Zx solid model (cm^3)	Zy solid model (cm^3)	Zx hollow model (cm^3)	Zy hollow model (cm^3)	CA (cm^2)	TA (cm^2)
Canis dirus **(USNM 8305, jaw length = 19.23 cm)**									
Post-M3	4.68	1.82	5.85	3.91	1.52	3.58	1.29	4.83	6.65
M2M3	4.34	1.84	6.75	3.40	1.44	2.98	1.37	4.40	6.17
M1M2	4.07	1.84	7.7	2.99	1.35	2.72	1.37	5.00	6.12
P4M1	3.89	2.13	11.06	3.16	1.73	2.39	1.36	4.20	6.02
P3P4	3.43	2.03	12.65	2.34	1.39	1.80	1.03	3.76	4.92
P2P3	3.41	2.09	-	2.39	1.46	1.70	0.92	3.43	4.76
Canine	3.64	3.53	16.86	4.59	4.45	3.58	3.42	8.23	8.34
Canis dirus **(USNM 8307, jaw length = 21.1 cm)**									
Post-M3	4.56	1.84	6.03	3.76	1.52	3.20	1.22	4.85	5.97
M2M3	4.45	1.86	6.6	3.62	1.51	2.95	1.07	4.36	5.70
M1M2	4.07	1.86	7.88	3.02	1.38	2.75	1.14	5.18	5.65
P4M1	3.8	1.95	11.4	2.76	1.42	2.19	1.25	4.60	5.63
P3P4	3.28	1.8	13.34	1.90	1.04	1.44	0.79	3.28	4.31
P2P3	3.12	1.72	-	1.64	0.91	1.37	0.69	3.01	3.93
Canine	3.16	2.88	18	2.82	2.57	2.28	1.90	6.07	6.07
Canis lupus **(USNM 274487, jaw length = 20.2 cm)**									
Post-M3	4.21	1.22	6.31	2.12	0.62	1.92	0.53	2.75	4.05
M2M3	4.14	1.22	6.91	2.05	0.60	1.93	0.49	2.72	4.01
M1M2	3.95	1.3	8.3	1.99	0.66	1.89	0.64	3.44	4.25
P4M1	3.91	1.75	11.05	2.63	1.18	2.07	0.88	3.61	4.93

P3P4	3.34	1.64	13.05	1.80	0.88	1.43	0.67	2.78	3.89
P2P3	2.99	1.46	-	1.28	0.63	1.01	0.52	2.57	3.19
Canine	3.18	2.72	17.68	2.70	2.31	1.82	1.63	5.13	5.50
***Canis lupus* (USNM 274942, jaw length = est. 19.7 cm)**									
Post-M3	4.07	1.57	5.87	2.55	0.98	2.00	0.72	2.91	4.80
M2M3	3.97	1.59	6.61	2.46	0.99	1.87	0.63	2.70	4.59
M1M2	3.74	1.61	7.64	2.21	0.95	1.66	0.77	3.45	4.67
P4M1	3.38	1.89	10.73	2.12	1.19	1.85	1.06	4.12	4.87
P3P4	2.91	1.74	12.54	1.45	0.86	1.22	0.75	2.83	3.76
P2P3	2.74	1.68	-	1.24	0.76	0.95	0.61	2.81	3.24
Canine	2.87	2.79	17.1	2.26	2.19	1.69	1.58	5.18	5.26
***Crocuta crocuta* (USNM 368502, jaw length = 18.5 cm)**									
Post-M1	5.31	1.4	5.75	3.88	1.02	3.71	0.74	4.61	5.36
P4M1	4.51	1.78	8.83	3.55	1.40	2.88	0.89	4.53	5.44
P3P4	4.14	1.84	11.1	3.10	1.38	2.74	1.21	5.19	5.82
P2P3	4.14	2.16	14	3.63	1.90	2.87	1.75	5.11	6.83
Canine	3.86	2.64	15.8	3.86	2.64	3.07	2.11	6.88	6.93
***Crocuta crocuta* (USNM 181524, jaw length = 18.43 cm)**									
Post-M1	4.82	1.32	6.3	3.01	0.82	3.00	0.76	4.25	4.91
P4M1	3.86	1.53	9.35	2.24	0.89	2.21	0.84	4.21	4.68
P3P4	3.32	1.7	11.38	1.84	0.94	1.74	0.92	4.25	4.40
P2P3	3.43	2.06	14.5	2.38	1.43	1.72	1.23	4.08	5.08
Canine	3.45	2.34	15.95	2.73	1.85	2.14	1.49	5.46	5.49
***Panthera leo* (USNM 162913,**									

jaw length = est. 22.7 cm)									
Post-M1	5.6	2.29	10.8	7.05	2.88	5.79	1.84	6.81	9.57
P4M1	5.02	2.27	13.5	5.62	2.54	4.45	2.21	6.31	8.81
P3P4	4.43	2.23	16.1	4.30	2.16	3.51	2.03	6.36	7.62
P2P3	4.47	2.14	-	4.20	2.01	3.14	1.69	4.89	7.35
Canine	5.31	3.65	21.2	10.10	6.95	7.45	5.35	12.41	12.79
***Panthera leo* (USNM 181569, jaw length = 21.97 cm)**									
Post-M1	5.12	2.02	10.06	5.20	2.05	4.61	1.28	5.66	7.70
P4M1	4.69	2.06	12.99	4.45	1.95	3.53	1.84	5.49	8.03
P3P4	4.33	2.12	15.32	3.90	1.91	3.12	1.89	6.05	7.20
P2P3	4.23	2.15	-	3.78	1.92	2.67	1.66	4.33	7.22
Canine	4.96	3.38	19.48	8.16	5.56	5.88	4.24	10.51	11.23
***Neofelis nebulosa* (USNM 49974, jaw length = 12.10 cm)**									
Post-M1	2.24	0.99	4.98	0.49	0.22	0.48	0.19	1.34	1.76
P4M1	2.22	1.18	6.37	0.57	0.30	0.48	0.26	1.77	2.01
P3P4	2.33	1.12	7.81	0.60	0.29	0.57	0.29	1.90	2.09
P2P3	2.51	1.14	-	0.71	0.32	0.57	0.26	1.55	2.23
Canine	2.83	1.66	10.55	1.31	0.77	1.29	0.75	3.65	3.72
***Neofelis nebulosa* (USNM 196600, jaw length = 10.96 cm)**									
Post-M1	1.99	0.89	4.5	0.35	0.15	0.34	0.14	1.16	1.40
P4M1	1.89	0.99	6.04	0.35	0.18	0.34	0.18	1.43	1.52
P3P4	1.93	1.01	7.46	0.37	0.19	0.32	0.16	1.32	1.45
P2P3	2.04	0.97	-	0.40	0.19	0.34	0.17	1.13	1.59
Canine	2.39	1.45	9.58	0.81	0.49	0.87	0.55	2.83	2.85

“L” is the distance between the articular condyle and the interdental gap. Jaw length was estimated for two specimens based on comparison with the conspecific individual. Section moduli (Z) for the “solid model” were calculated from the depth and width of the mandibular corpus measured on CT slices. Section moduli for the “hollow model”, cortical area (CA), and total area (TA) were calculated with the MomentMacro in ImageJ.

Table 2. Comparison of bite force estimates produced by various methods.

	Zx/L (this study)				Therrien (2005b)	Christiansen & Adolfsen (2005)	Wroe *et al.* (2005, sup. data)	Christiansen & Wroe (2007)	Thomason (1991) corrected bite force	Experimentally-determined bite force
Taxon	**Post-M1 hollow**	**P4M1 hollow**	**Post-M1 solid**	**P4M1 solid**	**P4M1 solid**	**Carn. (N)**	**Carn. (N)**	**Carn. (N)**	**Carn. (N)**	**Carn. (N)**
Canis dirus	0.35 (70%)	0.20 (68%)	0.39 (66%)	0.26 (70%)	0.22 (64%)	-	1577 (51%) Corrected 3479.4	-	-	
Canis lupus	0.22 (45%)	0.18 (60%)	0.26 (45%)	0.22 (58%)	0.17 (50%)	1262.3 (37%) Corrected 2786.5	1033 (33%) Corrected 2281.7	773.9 (38%) Corrected 1711.2	1412.2 (34%)	2000[a] (49%)
Crocuta crocuta	0.56 (112%)	0.28 (93%)	0.57 (98%)	0.31 (83%)	0.35 (104%)	1421.6 (42%) Corrected 3137.2	1569 (51%) Corrected 3461.8	985.5 (49%) Corrected 2177	-	4500[b] (108%)
Panthera leo	0.50 (100%)	0.30 (100%)	0.58 (100%)	0.38 (100%)	0.34 (100%)	3405.4 (100%) Corrected 7505	3085 (100%) Corrected 6800	2023.7 (100%) Corrected 4462.9	4167.6 (100%)	
Neofelis nebulosa	0.09 (17%)	0.07 (22%)	0.09 (15%)	0.07 (19%)	0.06 (19%)	587.8 (17%) Corrected 1301.5	1051 (34%) Corrected 2321.3	544.3 (27%) Corrected 1205.7	-	

Values in parentheses are relative bite force (i.e., expressed relative to the bite force of *Panthera leo*). For the bite force derived from the jaw musculature method, both published values and corrected values (if not published) are listed. "Carn." stands for estimates provided at the carnassial without precision of the exact position. [a]Nancy L. Denton, Purdue University, personal communication. [b]Binder and Van Valkenburgh (2000:fig. 3a).